Estimation of anisotropy parameters using the P-wave velocities on a cylindrical shale sample

Dariush Nadri[*1], *Joel Sarout*[1], *Andrej Bóna*[2], *and David Dewhurst*[1]

[1]*CSIRO Earth Science and Resource Engineering, Perth, Australia*
[2]*Department of Exploration Geophysics, Curtin University, Perth, Australia*

Summary

In this paper we present a new approach to the estimation of the Thomsen anisotropy parameters and symmetry axis coordinates from the P-wave traveltime measurements on cylindrical shale samples. Using the tomography-style array of transducers, we measure the ultrasonic P-wave ray velocities to estimate the Thomsen anisotropy parameters for a transversely isotropic shale sample. This approach can be used for core samples cut in any direction with regard to the bedding plane, since we make no assumption about the symmetry axis directions and will estimate it simultaneously with the anisotropy parameters. We use the very fast simulated re-annealing to search for the best possible estimate of the model parameters. The methodology was applied to a synthetic model and an anisotropic shale sample.

Introduction

Because of flat-lying sedimentation of clay particles, shales often behave as transversely isotropic (TI). Traditional computation of the Thomsen anisotropy parameters in a TI medium relays on a very few measurements of P-waves normal and along the bedding plane, and also one measurement at an oblique angle - often at 45° - to the bedding plane. This also requires measuring the shear wave velocities at normal to and along the bedding plane, which is always hard to do accurately. To avoid complications that may arise from the tilting of the symmetry axis, hence satisfying the VTI or HTI assumptions, majority of shale samples are cored either normal to or along the bedding planes. Within these assumptions, one can simply use the phase or ray velocity equations for a transversely isotropic medium to estimate the anisotropy parameters. Sometimes it is difficult or impossible to obtain cores along these directions such as for deviated wells or for the dipping formations. In laboratory experiments where the acoustic measurements are taken under non-isotropic stress field, the symmetry axis direction may also changes which may violates the transverse isotropy assumption with vertical or horizontal symmetry axis direction. These considerations motivate us to take into account the symmetry axis deviations from normal to the bedding planes, which not only brings more freedom to laboratory acoustic experiments but also allows for tracking the possible change of the symmetry axis during measurements under stress. Here, we use a tomography-style geometry of transducers to measure the ultrasonic ray velocity in a cylindrical sample (Figure 1). We developed a ray-tracing based algorithm to compute the ray velocities, assuming homogeneity of the sample. Using these velocities, we estimate the Thomsen anisotropy parameters and the symmetry axis coordinates using the Very fast simulating re-annealing (VFSR) algorithm by searching for the true solution, and where required, implementing a non-linear conjugate gradient (CG) algorithm to tune the best estimate. We applied the methodology to a synthetic model and a real shale sample.

Methodology

To compute the phase velocity we use the parametric solution of the Christoffel equation for a homogenous transverse isotropic medium with vertical symmetry axis given by Ursin and Stovas (2006),

$$1/v^2 = 1/\alpha_0^2 - p^2(\sigma+\delta) - (\gamma^2-1)\left[\sqrt{1+bp^2\alpha_0^2+cp^4\alpha_0^4}-1\right]\Big/2\alpha_0^2$$

$$, b = -\frac{4}{\gamma^2-1}(\sigma-\delta),\ c = 4\left[2(\gamma^2-1)\sigma/\gamma^2+(\sigma+\delta)^2\right]\Big/(\gamma^2-1)^2,$$

$$\gamma = \frac{\alpha_0}{\beta_0},\ \sigma = \gamma^2(\varepsilon-\delta), \qquad (1)$$

where v is the phase velocity, p is the ray parameter (projection of slowness vector to the bedding plane) and α_0, β_0, ε, and δ are the Thomsen anisotropy parameters; the anisotropy parameters α_0 and β_0 are the P- and S-waves velocities along the symmetry axis.

Because of the relatively small size of the transducers, the measured velocity is the ray velocity (Vestrum, 1994). The magnitude of the ray velocity is related to the phase velocity,

$$V^2 = v^2 + (\partial v/\partial\theta)^2, \qquad (2)$$

where V is the P-wave ray velocity and θ is the phase angle. The derivative $\partial v/\partial\theta$ can be expressed as a function of the ray parameter,

$$\frac{\partial v}{\partial\theta} = \frac{\sqrt{1-p^2v^2}\,\partial v/\partial p}{v + p\,\partial v/\partial p}, \qquad (3)$$

where the derivative $\partial v/\partial p$ can be computed from equation 1.

For a shale sample that is not plugged in direction normal to the bedding plane computing the ray velocity for the rays

not propagating in the symmetry plane is not as straightforward as for rays propagating in the symmetry plane – the effect of tilting the symmetry axis should be considered. Figure 2 shows the configuration of a ray propagating off the symmetry plane. All the ray, slowness, and symmetry axis vectors are in a plane. For a given ray path, the ray angle can be written as a function of other geometrical parameters as,

$$\cos\psi = \sin\beta\cos\alpha\sin\omega + \cos\beta\cos\omega$$
$$\alpha = \varphi - \tilde{\alpha}, \qquad (4)$$

where ψ is the ray angle, β is the ray incidence angle, ω and φ are symmetry axis coordinates, and $\tilde{\alpha}$ is the ray azimuth.

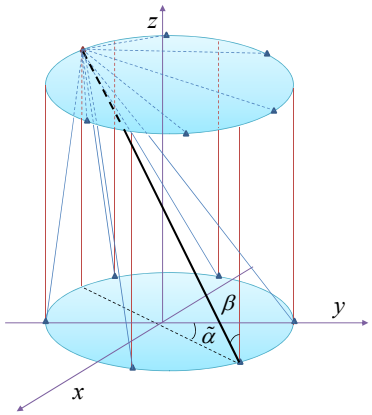

Figure 1: A schematic of ray shooting configuration for an array of source and receivers on a cylindrical shale sample. Each transducer acts as a source while the rest of the transducers act as receivers.

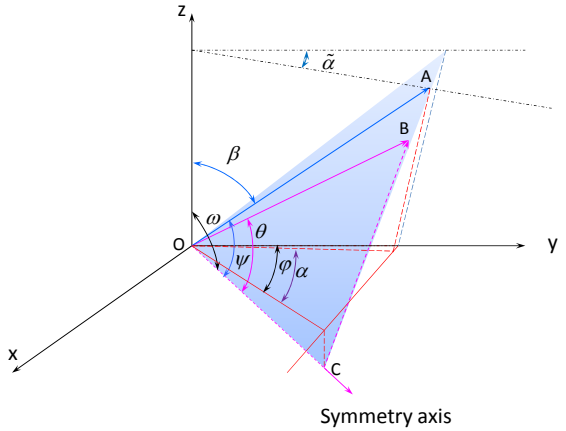

Figure 2: A schematic of ray (OA), slowness (OB), and symmetry axis (OC) vectors. CB is the projection of slowness vector on the isotropy plane and is the horizontal slowness (after Tsvankin, 1997 with modification).

To relate the ray and phase angles, one can write the ray angle in terms of the ray parameters (see e.g. Ursin and Stovas, 2006),

$$\tan\psi = \frac{pv^3 + \partial v/\partial p}{v^2\sqrt{1-p^2v^2}}, \qquad (5)$$

Having the ray angle for a given configuration and a media with given anisotropy parameters and symmetry axis coordinate one can find the ray parameter p using ray tracing.

Before attempting to compute the ray parameter, we check whether the ray path is within the isotropy plane. To do this we check whether the ray vector is parallel to the symmetry axis,

$$\vec{R} = \hat{i}\sin\beta\sin\tilde{\alpha} + \hat{j}\sin\beta\cos\tilde{\alpha} + \hat{k}\cos\beta, \qquad (6)$$
$$\vec{A} = \hat{i}\sin\omega\sin\varphi + \hat{j}\cos\omega\cos\varphi + \hat{k}\sin\omega, \qquad (7)$$
$$\vec{R}\cdot\vec{A} = 0, \qquad (8)$$

where $\vec{R}$ and $\vec{A}$ are vectors parallel to ray and symmetry axis, respectively.

Ray tracing in TTI media

The simplest way to compute the ray parameter is to use equation 5. To avoid confusion about the sign of the root square we square the equation 5 and write it in the following form,

$$f = \left(pv^3 + \partial v/\partial p\right)^2 - v^4\left(1-p^2v^2\right)\tan^2\psi, \qquad (9)$$

This approach is fast and works well for most of the cases where the anisotropy parameters are within the realistic values and for the rays propagating not very close to the isotropy plane. It has only one root for the above conditions and it can be found for example using the Newton-Raphson method (see e.g. Press et al., 2007).

For the odd values of the anisotropy parameters and where the ray propagates close to the isotropy plane, it is hard to bracket the equation 9 which means that other alternatives should be sought. One approach is to use an optimization algorithm to minimize for example an objective function of the ray angle with respect to ray parameter,

$$g = \left(\cos^2_m\psi - \cos^2_c\psi\right)^2, \qquad (10)$$

where m and c stand for the measured and computed ray angles using the equations 4 and 5, respectively. We use the Newton method to minimize the above objective function. In extremely rare conditions we realized that equation 10 may not be convex for the rays propagate very close to isotropy plane, hence the minimum is very close to the upper boundary of the equation 10 and bi-sectioning techniques may fail. The upper boundary is indeed the inverse of the slowness vector (see e.g. Thomsen, 1986),

$$\frac{1}{p^2} = \alpha_0^{\,2}\left(1+\varepsilon+\Delta\right),$$

$$\Delta = 0.5\left(1-\beta_0^{\,2}/\alpha_0^{\,2}\right)\left[\sqrt{1+\frac{4\left(1-\beta_0^{\,2}/\alpha_0^{\,2}+\varepsilon\right)\varepsilon}{\left(1-\beta_0^{\,2}/\alpha_0^{\,2}\right)^2}}-1\right]. \quad (11)$$

To tackle this issue, we set the ray parameter to the upper bound and decrease it exponentially while evaluating the equation 10. After a few iterations it reaches the minimum of the equation 10. In any of the above approaches we always use a random ray parameter drawn from a uniform distribution to start with.

Minimization of anisotropy parameters

To find the anisotropy parameters, ε, δ, α_0, and β_0 we form an objective function of the P-wave ray velocities and minimize it using Very fast simulating re-annealing algorithm (Ingber, 1989) t,

$$\phi = \frac{1}{2}\left(\mathbf{V}-\mathbf{V}'\right)\left[\mathbf{C_D}\right]^{-1}\left(\mathbf{V}-\mathbf{V}'\right)^T, \quad (12)$$

where ϕ is the objective function and $\mathbf{V}$ is the vector of the ray velocities from all the source-receiver pairs. $\mathbf{C_D}$ is the covariance matrix of the errors in the ray velocity measurements, and T denotes the transpose. The diagonal elements are variances and are the same for all the measurements. Assuming there is no correlation among the residual errors of the ray velocities, the off-diagonal elements (covariance) of the matrix $\mathbf{C_D}$ are zero. Where required, we also apply a non-linear conjugate gradient algorithm after Very fast simulating re-annealing, to guarantee the convergence to the true solution. Both minimization algorithms require the derivatives of the objective function with respect to the model parameters, namely,

$$\frac{\partial\phi}{\partial m_j} = -\frac{\partial\mathbf{V}}{\partial m_j}\left(\mathbf{V}-\mathbf{V}'\right),$$

$$\frac{dV}{dm} = \frac{\partial V}{\partial m}\bigg|_{p=cons.} + \frac{\partial V}{\partial p}\frac{dp}{dm},\ m \to \alpha_0, \beta_0, \varepsilon, \delta \quad (13)$$

$$\frac{dp}{dm} = -\frac{\partial\cos\alpha/\partial m\big|_{p=cons.}}{\partial\cos\alpha/\partial p}.$$

The derivatives of the ray velocity with respect to the model parameters and the ray parameter can be derived from the equations 1-3. In contrary to our previous approach to compute the dp/dm (Nadri et al., 2011), where we used the derivatives of source- receiver offset with respect to either model parameters in a constant ray parameter or ray parameter which requires Δz -the difference in source-receiver locations along the z axis and will be zero if they are in the same level-, here we take the derivatives with respect to cosine of azimuth (φ) which can be easily derived from equation 4. The connection of azimuth (φ) with both model parameters and ray parameter come through the ray angle (ψ) in equation 5.

The derivatives of the ray velocity with respect to the symmetry axis coordinates can be computed as,

$$\frac{dV}{d\varphi} = \frac{dV}{dp}\left(\frac{d\psi}{dp}\right)^{-1}\frac{d\psi}{d\varphi}, \quad (14)$$

$$\frac{dV}{d\omega} = \frac{dV}{dp}\left(\frac{d\psi}{dp}\right)^{-1}\frac{d\psi}{d\omega}, \quad (15)$$

where $d\psi/dp$, $d\psi/d\alpha$, and $d\psi/d\omega$ can be computed from the equations 5 and 4, respectively. For a ray propagating in the isotropy plane, the derivatives of the ray velocity with respect to the anisotropy parameters can be computed from equation 11 directly which is also zero with respect to the Thomsen anisotropy parameter δ and the symmetry axis coordinates.

Examples

As the first example to test the algorithm, we computed the ray velocity for 110 different ray paths for a synthetic sample with anisotropy parameters and symmetry axis coordinates given in Table 1. We continued the VFSR minimization up to 2000 iterations (annealing temperature) with 100 model selections at each temperature. A reasonable lower and upper limit for the anisotropy parameters was set (Table 1) and model parameters were randomly drawn from the uniform distribution. Also, minimization always started from a random prior within the boundaries. The annealing parameters, temperature and decays, were set to 1000 and 0.9 for all the model parameters, respectively. CG started with a prior model set at the best solution from the VFSR and continued up to 20 iterations. Table 1 show that VFSR has reached closely to the exact solution, whereas the CG reached the true solution. Figure 3 shows the evolution of the objective function from the CG. After a few iterations, residual error has dropped significantly.

The measurement system consists of a multi-channel ultrasonic monitoring equipment attached to a triaxial cell. An array of 16 newly designed miniature ultrasonic P-wave transducers of 5mm diameter (Sarout et al., 2010) with the central frequency of 500KHz is directly attached to the lateral surface of the cylindrical shale sample through a Viton sleeve. This sleeve aims to (i) isolate the specimen from the medium (hydraulic oil), and (ii) control the pore fluid pressure independently from the applied triaxial stresses. In this example data corresponds to a survey performed at 45MPa confining pressure and 5MPa pore

pressure. Figure 4 shows an array of waveforms shot from a transducer and recorded at the 15 other transducers before and after applying a Butterworth Bandpass filter in the range of 2-800KHz. In some cases, where the first arrival overlaps with a strong electromagnetic system noise (Figure 4 top), Bandpass filtering distorts the P-wave arrival and makes it hard to pick accurately. We picked 204 traveltimes and computed the correspondent ray velocities. Out of 204 ray paths, less than half of the measurements were actually recorded from the reciprocal pairs of the transducers. These repetitive measurements were averaged before preceding the minimization. Data were extremely noisy so we have to put a cut off after 1500 iterations in which only the measurements with the residual errors less than 10 percent were allowed to continue for the rest of 1000 iterations. The estimated parameters for the best solution from the VFSR are shown in Table 1. The high level of noise in the traveltime measurements are mostly due to adjacent source – receivers and the pairs of the transducers which are aligned in one side of the cylinder.

Parameter	Lower	Upper	True	VFSR	CG	VFSR
ε	0	1.0	0.20	0.185	0.20	0.25
δ	-0.3	0.8	0.15	0.152	0.15	0.18
α_0	1	6	2.50	2.50	2.50	3.20
β_0	0.5	3	1.50	1.53	1.53	2.07
φ	0	180	45	45.1	45.0	127
ω	0	180	120	120.2	120.0	150

Table 1: The second and third columns show the hard constraint during the minimization. The columns in purple show the true model, the best estimate from the VFSR, and the estimate from the CG for the synthetic model. The column in blue shows the best estimates from the shale sample. The anisotropy parameters α_0 and β_0 are given in km/sec.

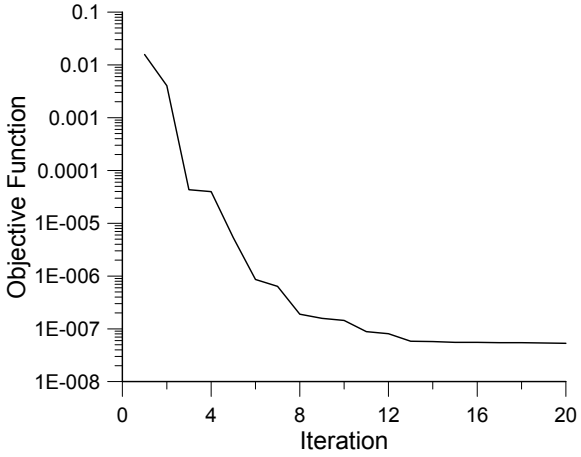

Figure 3: Convergence rate of the objective function from the minimization using the conjugate gradient.

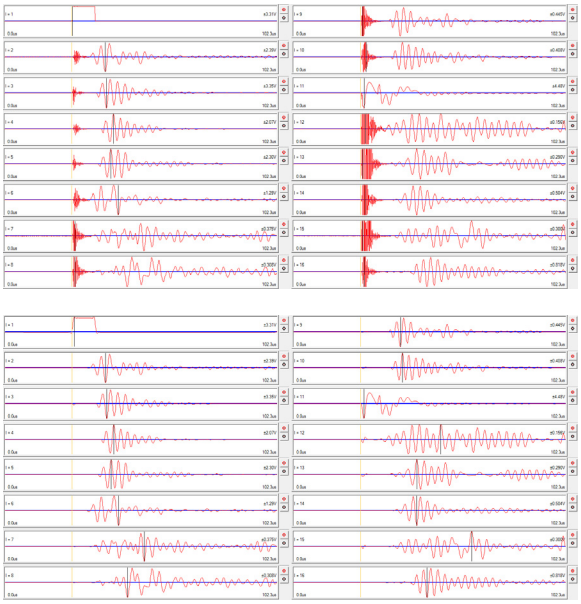

Figure 4: A waveform array shot from one transducer and recorded in 15 others transducers before (above) and after Bandpass filtering (below). To improve the signal to noise ratio each shot has been 50 times repeated and stacked at each receiver. The first panel at top left in each figure shows the source signature which is a tapered box function.

Conclusions

Using an array of 16 newly designed piezoelectric acoustic transducers, we measured the P-wave ray velocities from different combinations of transducer pairs under the directional stresses. Because of very small sensitivity of the P-wave ray velocity to β_0, we do not expect to resolve it from the VFSR in real experiments, however because the ray velocities from the synthetic model are noise free, CG was able to resolve it fairly well. This shows that the objective function in the model space has a unique solution and the anisotropy parameters can be estimated independently. Also in the first example the rest of the anisotropy parameters resolved well, in particular the azimuth and polar angle of the symmetry axis resolved to the true values in both VFSR and CG algorithms. The ray tracing is extremely fast, in particular using the root-finding approach. There is no assumption of weak anisotropy in any of the equations and neither ray tracing nor minimization fail for the strongly anisotropic samples. Despite the stochastic nature of Very fast simulated re-annealing which takes two orders of million function evaluations, minimization only takes less than 5 minutes on a Quad core Intel processor X5570 series using a serial programming code written in C++.

EDITED REFERENCES

Note: This reference list is a copy-edited version of the reference list submitted by the author. Reference lists for the 2011 SEG Technical Program Expanded Abstracts have been copy edited so that references provided with the online metadata for each paper will achieve a high degree of linking to cited sources that appear on the Web.

REFERENCES

Ingber, L., 1989, Very fast simulated reannealing: Mathematical and Computer Modeling, **12**, no. 8, 967–973, doi:10.1016/0895-7177(89)90202-1.

Nadri, D., J. Sarout, A. Bóna, and D. Dewhurst, 2011, Estimation of Thomsen anisotropy parameters using the P-wave velocities on a cylindrical shale sample: 73rd Annual International Conference and Exhibition, EAGE, Extended Abstracts, C023.

Press, W. H., S. A. Teukolsky, W. T. Vetterling, and B. P. Flannery, 2007, Numerical recipes: The Art of Scientific Computing: Cambridge University Press.

Sarout, J., A. Ougier-Simonin, Y. Guéguen, and A. Schubnel, 2010, Active and passive seismic monitoring of shales under triaxial stress conditions in the laboratory: EAGE Shale Workshop: Shale — Resource and Challenge.

Thomsen, L., 1986, Weak elastic anisotropy: Geophysics, **51**, 1954–1966, doi:10.1190/1.1442051.

Tsvankin, I., 1997, Reflection moveout and parameter estimation for horizontal transverse isotropy: Geophysics, **62**, 614–629, doi:10.1190/1.1444170.

Ursin, B., and A. Stovas, 2006, Traveltime approximation for a layered transversely isotropic medium: Geophysics, **71**, no. 2, D23–D33, doi:10.1190/1.2187716.

Vestrum, R. W., 1994, Group- and phase-velocity inversions for the general anisotropic stiffness tensor: M.S. thesis, University of Calgary.